THE JOURNAL OF PHYSICAL CHEMISTRY Letters

pubs.acs.org/JPCL

Secondary Structure of Ac-Ala$_n$-LysH$^+$ Polyalanine Peptides (n = 5,10,15) in Vacuo: Helical or Not?

Mariana Rossi,*,† Volker Blum,† Peter Kupser,† Gert von Helden,† Frauke Bierau,† Kevin Pagel,‡,§ Gerard Meijer,† and Matthias Scheffler†

†Fritz-Haber-Institut der Max-Planck-Gesellschaft, D-14195 Berlin, Germany, and ‡Freie Universität Berlin, Institut für Chemie und Biochemie, D-14195 Berlin, Germany

ABSTRACT The polyalanine-based peptide series Ac-Ala$_n$-LysH$^+$ (n = 5−20) is a prime example that a secondary structure motif that is well-known from the solution phase (here: helices) can be formed in vacuo. Here we revisit the series members n = 5,10,15, using density functional theory (van der Waals corrected generalized gradient approximation) for structure predictions, which are then corroborated by room temperature gas-phase infrared vibrational spectroscopy. We employ a *quantitative* comparison based on Pendry's reliability factor (popular in surface crystallography). In particular, including *anharmonic* effects into calculated spectra by way of ab initio molecular dynamics produces remarkably good experiment−theory agreement. We find the longer molecules (n = 10,15) to be firmly α-helical in character. For n = 5, calculated free-energy differences show different H-bond networks to still compete closely. Vibrational spectroscopy indicates a predominance of α-helical motifs at 300 K, but the lowest-energy conformer is not a simple helix.

SECTION Biophysical Chemistry

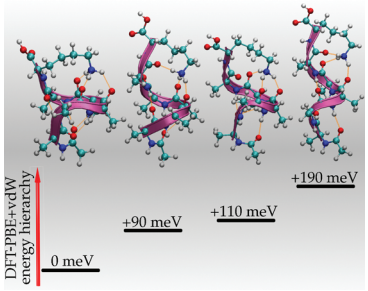

Many factors act together to determine the structure of peptides and proteins, and it is crucial to understand each of them in detail for a truly predictive picture of the whole. Solvent effects are often emphasized as indispensable, and they certainly play a key role in structure formation, especially at the tertiary and quarternary level (although intact, solution-phase formed tertiary/quarternary structure can apparently be *transferred* into the gas phase; see ref 1 and references therein). On the other hand, the *secondary* structure level (helices, sheets, turns) is heavily influenced by *intramolecular* interactions — most importantly, hydrogen bonds. For this subset of interactions, benchmark experiment−theory comparisons under well-defined "clean-room" conditions in vacuo can furnish critical information toward a complete, predictive picture of peptide structure and dynamics, *if the same structure as in the solution phase can be formed*. For example, first-principles approaches such as density functional theory (DFT) with popular exchange-correlation functionals do not account for van der Waals (vdW) interactions, and precise experimental calibration points for different, actively developed theoretical remedies[2−7] would be extremely useful.

In a seminal ion-mobility spectrometry study more than a decade ago, Hudgins, Ratner, and Jarrold (HRJ)[8] reported the formation of just such a secondary structure motif (helical) known from the solution phase in vacuo for a series of designed, charged polyalanine-based peptides Ac-Ala$_n$-LysH$^+$ (n = 5−20). While much follow-up work has been done after the original HRJ study (e.g., refs 9−16) the "helical" nature of the exact series Ac-Ala$_n$-LysH$^+$ is so far still established only indirectly by comparing ion-mobility cross sections to results from force-field-based molecular dynamics. A helical assignment for polyalanine is thus plausible and easily accepted, but different structural conclusions are not entirely ruled out. Additional ion-mobility experiments with microsolvation[11] indicate that the secondary structure is not yet helical for n < 8. On the other hand, a spectroscopic study of Ac-Phe-Ala$_5$-LysH$^+$[14] inferred structures with "helical" H-bond rings (α- or 3_{10}-helix-like) as the dominant conformers.

The key goal of the present work is to verify the structure of the n = 5, 10, and 15 members of the original HRJ series, both experimentally and theoretically. This is an important task, as *safely* knowing the correct structure is crucial for any further physical conclusions — particularly for a benchmark system such as the HRJ series. On the theory side, we employ DFT in the PBE[17] generalized gradient approximation corrected for vdW interactions,[6] which are critical to guarantee the necessary accuracy for our work. We confirm the helical assignment for n = 10 and 15. For n = 5, the lowest energy structure is indeed not a simple helix. Even for such a relatively short peptide, there is an enormous structural variety to navigate.[14,15,18] Harmonic free-energy calculations show that multiple conformers for n = 5 (both helical and nonhelical) should coexist

Received Date: October 11, 2010
Accepted Date: November 19, 2010
Published on Web Date: December 01, 2010

at $T \approx 300$ K. Importantly, all our findings are underpinned by quantitatively comparing experimental infrared multiphoton dissociation (IRMPD) and calculated vibrational spectra in the 1000−2000 cm^{-1} region. Since these spectra [measured at $T \approx 300$ K, and calculated including finite T anharmonic effects through ab initio molecular dynamics (AIMD)] are continuous, we employ John Pendry's reliability factor R_P,[19] widely used in the same context in low-energy electron diffraction (LEED) surface crystallography,[20] for an unbiased experiment-theory comparison, using a program distributed with ref 21. This quantitative measure demonstrates beyond doubt the superiority of molecular dynamics-derived theoretical spectra over single-point spectra in the harmonic approximation, and quantitatively corroborates our theoretical structural predictions.

The Pendry reliability factor[19] used to quantify experiment−theory agreement of essentially continuous spectra is well established in LEED.[20,21] It precisely addresses our need to match mainly peak positions, rather than, say, a simple overall square-of-intensity comparison, which would overemphasize a few large intensity peaks (amide-I and -II) over the many small, structure-sensitive features in other regions (e.g., amide-III).[22,23] Given two continuous curves $I_{exp}(\omega)$ and $I_{th}(\omega)$, sensitivity to peak positions is achieved by comparing renormalized logarithmic derivatives of the intensity: $Y(\omega) = L^{-1}(\omega)/[L^{-2}(\omega) + W^2]$, with $L(\omega) = I'(\omega)/I(\omega)$ and W approximately the half width of peaks in the spectra (here taken to be 10 cm^{-1}), so that $R_P = \int d\omega (Y_{th} - Y_{exp})^2/(Y_{th}^2 + Y_{exp}^2)$. In practice, this convention leads to $R_P = 0$ for perfect agreement, 1 for uncorrelated spectra, and 2 for perfect anticorrelation. In LEED, $R_P \approx 0.3$ is usually taken to be acceptable experiment-theory agreement. Since R_P is sensitive to small wiggles, experimental noise in low-intensity regions must be removed, which is here achieved by splining and gently smoothing (3-point formula) the raw data before interpolation onto a fine numerical grid, just like in LEED.[20] R_P is always determined including a rigid shift Δ of all calculated frequencies, but no scaling factors. Rigid shifts of calculated IR spectra including anharmonicity compared to experiment have been described before,[24] and most likely reflect a small, systematic mode softening due to the density functional used.

We first focus on the larger molecules, $n = 10$ and 15, where all available evidence points to helical structure. An exhaustive structure search, similar to that for $n = 5$ explained further below, is impractical for such large molecules, but we have performed similar exhaustive searches for $n = 4$−8. A crossover to α-helical lowest-energy conformers occurs at $n = 7$ (unpublished results). In Figure 1a,b, we first demonstrate the structure sensitivity of our spectra by comparing *harmonic* spectra (convoluted with a Gaussian function to account for experimental broadening, see Experimental and Computational Section) for 3_{10} and α-helical conformations to experiment. Both the visual comparison (incorrect relative peak positions in 3_{10}, particularly note the differences in the amide-III region between 1000 and 1400 cm^{-1}) and R_P clearly favor α, although at $R_P = 0.46$, the α-helical assignment is only qualitatively clear. This situation drastically changes when considering AIMD-derived calculated intensities instead, which include anharmonic effects, in Figure 1c. Not only is $R_P = 0.32$ noticeably improved, but also the

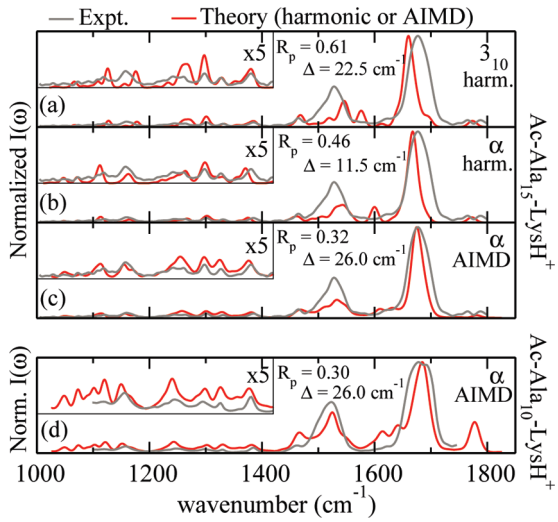

Figure 1. Comparison between experimental [gray lines] and theoretical [red lines] vibrational spectra, all normalized to 1 for the highest peak. (a,b) Ac-Ala_{15}-$LysH^+$: calculated spectra based on the harmonic approximation, for a 3_{10}-helical (a) and an α-helical (b) local minimum of the potential energy surface. (c) Ac-Ala_{15}-$LysH^+$: calculated spectrum from AIMD (including anharmonic effects), starting from an α-helix and α-helical in character throughout the simulation. (d) Same as panel c, for Ac-Ala_{10}-$LysH^+$. Pendry R-factors and rigid shifts Δ (see text) between measured and calculated spectra are included in each graph (calculated spectra are shifted by Δ for visual comparison).

visual comparison of all relative peak positions is remarkably better. Obviously, some residual quantitative uncertainties remain (e.g., in the region of 1450−1600 cm^{-1}), which must be expected due to residual errors of any approximate density functional. In addition, we are still comparing calculated linear absorption spectra with experimental IRMPD (multiphoton absorption) spectra. While it has been shown that IRMPD spectra can come close to the linear absorption spectra,[25] differences, especially in relative peak intensities, can remain. These points considered, the agreement is remarkable. The situation is similar (even slightly better) for $n = 10$, with $R_P = 0.30$ (Figure 1d). We note additionally that initial, locally stable 3_{10} arrangements morph to α after only a few picoseconds of AIMD, and that α-helix conformations are structurally stable even at high T,[26] in AIMD at 500 K for at least several tens of picoseconds;[27] for $n = 10$ and 15, 3_{10} helical local energy minima are higher in energy than α by at least 0.41 and 0.82 eV, respectively. All available evidence thus points to α-helical secondary structure for $n = 10$, 15. To be as specific as possible, this means that the H-bond networks of the entire molecules remain substantially α-helical even in the dynamic situation reflected in our MD simulation, even if individual H-bonds, especially near the terminations, may be connected differently at times. A detailed account of the development of the H-bond network for $n = 15$ throughout the *NVE* trajectory that led to Figure 1c is given in the Supporting Information.

For Ac-Ala_5-$LysH^+$, the situation is less clear in the literature,[8,11] and we proceed with a detailed structure search as follows: We first generate a large body of possible starting conformations using the empirical OPLS-AA force field (ref 28

DOI: 10.1021/jz101394u | J. Phys. Chem. Lett. 2010, 1, 3465–3470

and references therein) in a series of basin hopping structure searches performed with the TINKER[29] package. Our particular choice of force field was not motivated by any other reason than that an input structure "generator" for DFT was needed. That said, OPLS-AA for gas-phase alanine dipeptides and tetrapeptides was assessed rather favorably in earlier benchmark work.[30,31] In the searches, specific constraints on one or more hydrogen bonds could be enforced. In total, we collected $O(10^5)$ nominally different conformers from (i) an unconstrained search, (ii) one hydrogen bond in the Ala_5 part constrained to remain α-helical, (iii) two hydrogen bonds in Ala_5 constrained to form a 3_{10}-helix, (iv) three hydrogen bonds in the Ala_5 part constrained to form a 2_7 helix, or (v) one hydrogen bond in the full peptide constrained to a π-helical form. As is well-known,[32] conformational energy differences between different types of secondary structure may vary strongly between different force fields and/or DFT. We reduce our reliance on the energy hierarchy provided by the force field by following up with full DFT+vdW relaxations for a wide range of conformers, 302 in total. This range includes the lowest ~0.35 eV for the unconstrained and α-helical searches, and the lowest ~0.15 eV for the 3_{10}-constrained search, as well as the lowest few π- and 2_7-helical candidates. Almost all π-helical geometries found in the force-field relaxed with DFT either into α or 3_{10} helices, and all relaxed 2_7 helices were higher in energy than our lowest-energy conformer by at least 0.26 eV.

All distinct local structural minima of Ac-Ala_5-$LysH^+$ in DFT+vdW were characterized according to their overall H-bond patterns (other differences, such as the exact orientation of the Lys side chain or the COOH group near the C terminus, can still lead to several shallow local structure minima within each H bond pattern). Four characteristic low-energy H-bond networks (the lowest-energy structure minima for each) are shown in Figure 2. Three of them (labeled α-1, α-2, and 3_{10}-1) are "helical" in the sense that they contain two well-separated terminations with the appropriate α- or 3_{10}-like H-bond loops in their Ala_5 section. The fourth, however, labeled g-1, is our *overall* lowest-energy conformer, and is *not* "helical" in the same sense. In particular, it contains one H-bond (O-5 to NH-2) that runs *against* the normal helix dipole, effectively short-circuiting the terminations. In fact, several small variations of local structure minima with that same "inverted" H-bond exist, which are all lower in energy than the "properly" helical conformer α-1.

In Table 1, we summarize the computed energy hierarchy for the conformers of Figure 2. In DFT-PBE+vdW, the g-1 conformer is more stable than its closest competitors by 0.1−0.2 eV. On this scale, vdW interactions are important, as seen by comparing to the pure DFT-PBE energy hierarchy (no vdW). On the other hand, finite temperature effects reduce the relative stability of g-1. The calculated harmonic free energy of g-1 and α-1 at 300 K is almost equal, and α-2 is only slightly (~60 meV) less stable; only 3_{10}-1 stays noticeably removed. The expected stability of at least three out of the four conformers is thus similar, and at room temperature we would expect all of them to be present or even interconvert in experiment. We note in passing that the hierarchy for other DFT functionals (revPBE, or B3LYP at fixed geometry obtained

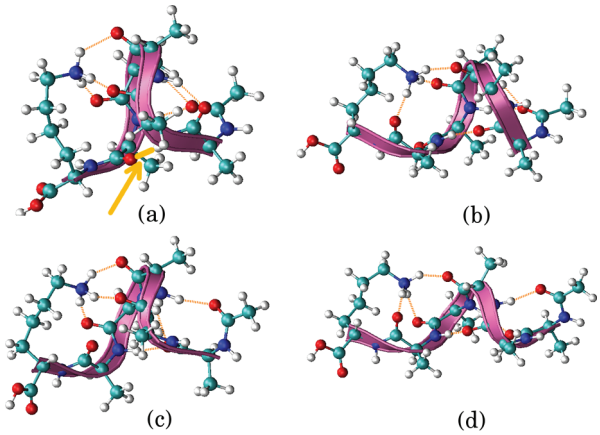

(e)	g-1	α-1	α-2	3_{10}-1
O(Ac)	NH-4(α) NH-5(π)	NH-3(3_{10}) NH-4(α)	NH-3(3_{10})	NH-3(3_{10})
O-1	NH-3(2_7)	NH-5(α)	NH-4(3_{10}) NH-5(α)	NH-4(3_{10})
O-2	NH_3^+	NH_3^+	NH_3^+	NH-5(3_{10})
O-3	NH_3^+	NH_3^+	NH_3^+	NH_3^+
O-4	NH_3^+	NH-6	NH_3^+	NH_3^+
O-5	**NH-2**	NH_3^+	NH_3^+ weak	NH_3^+

Figure 2. Visualization of low-energy Ac-Ala_5-$LysH^+$ conformers: (a) g-1, with the H-bond against the helix dipole highlighted in yellow and pointed to by the arrow (see text); (b) α-1; (c) α-2; (d) 3_{10}-1. (e) H-bond networks associated with each conformer. (C−)O and N−H groups are numbered starting from the N terminus and ending at the C terminus.

Table 1. Energy Differences of the Four Chosen Ac-Ala_5-$LysH^+$ Conformers with Respect to g-1: Pure DFT-PBE (No vdW), DFT-PBE+vdW (PES Only), and DFT-PBE+vdW Harmonic Free Energy ΔF at 300 K[a]

	g-1	α-1	α-2	3_{10}-1
DFT-PBE	0.0	0.04	0.08	0.04
DFT-PBE+vdW	0.0	0.09	0.11	0.19
ΔF(300 K)	0.0	0.01	0.06	0.17

[a] All energies in electron volts.

using the PBE functional) is qualitatively similar, as long as a vdW correction is included.[33]

Interestingly, the termination-connecting H-bond of the g-1 conformer leads to a somewhat smaller overall volume of g-1 compared to the α-1, α-2, or 3_{10}-1 conformers. This is quantified in Figure 3 by way of computed relative ion-mobility cross sections (using an empirical rare gas−molecule interaction potential[34]). We show $\Omega = (\Omega_{measured} - 14.50n\,Å^2)$ as a function of peptide chain length n, the same expression used by HRJ.[8] Remarkably, the g-1 conformer for $n = 5$ together with α-helical conformers for $n = 10$ and 15 (red dashed line) yields exactly the same qualitative behavior as the original data of HRJ. In contrast, our α-1 and α-2 conformers would yield a much shallower drop toward $n = 5$. The 3_{10}-1 conformer ends up too high.

Finally, Figure 4a−d shows computed anharmonic vibrational spectra for all four conformers compared to experiment, with the respective R_p factors and shifts. As $I(\omega)$ values are derived from AIMD trajectories, different conformers could conceivably interconvert over time, regardless of the

DOI: 10.1021/jz101394u | J. Phys. Chem. Lett. 2010, 1, 3465–3470

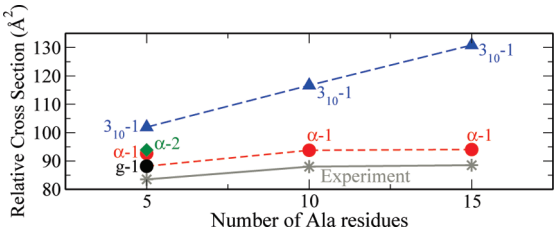

Figure 3. Ac-Ala$_n$-LysH$^+$, n = 5,10,15: Calculated (using an empirical rare gas−molecule interaction potential[34]) ion-mobility cross sections and comparison with experiment (ref 8). Blue triangles correspond to conformers in the 3_{10}-1 geometry, red circles correspond to conformers in the α-1 geometry, the black circle corresponds to the g-1 conformer, the green diamond corresponds to the α-2 conformer, and gray stars correspond to the experimental data from ref 8. The solid and dashed lines serve only as a guide to the eye, and have no physical significance.

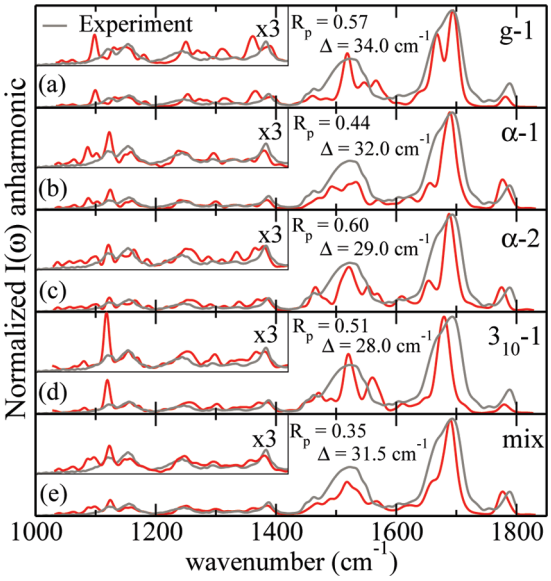

Figure 4. Ac-Ala$_5$-LysH$^+$: (a−d) Theoretical anharmonic vibrational spectra from AIMD trajectories (red lines) for the four chosen conformers of Figure 2, compared with experiment (gray line); (e) optimum calculated spectrum when assuming a coexistence of more than one conformer in experiment. Pendry R-factors and rigid shifts Δ (see text) between measured and calculated spectra are included in each graph (calculated spectra are shifted by Δ for visual comparison). All spectra have been normalized to 1 for the highest peak.

starting structure. In fact, an interconversion happens for short periods between α-1 and α-2, which we still label for the initial (and predominant) conformation.

For separate trajectories a−d, we do find visually reasonable agreement and somewhat reasonable R_P-factors (between 0.44 and 0.60) when comparing experiment and anharmonic spectra. 3_{10}-1 is visually set apart by the unsatisfactory relative position of its amide-I peak, but there are otherwise no unambiguous contradictions between experiment and theory. Purely harmonic spectra are again significantly worse, both visually (not shown) and based on high R_P-factors between 0.66 and 0.79. Nonetheless, even the "anharmonic" agreement is not as good as for n = 10 and n = 15, and our harmonic free-energy estimate above already indicates a reason: One would expect a mix of conformers, and not just a single one, to contribute to the gas-phase sample. To illustrate this point, Figure 4e shows the result of simply linearly averaging theoretical spectra, with mixing factors derived by minimizing R_P. The result, in our view, is remarkable. The "optimum" theoretical spectrum achieves R_P = 0.35, with convincing visual agreement to experiment in the details. One might be inclined to dismiss this as the predictable outcome of a fit, but in addition, the computed optimum fractions are 25% g-1, 60% α-1, 15% α-2, and *no* contribution from 3_{10}-1 at all. This coincidence with our free-energy based conclusions strengthens our confidence in the results of our structural search significantly.

In summary, the lowest-energy conformer of Ac-Ala$_5$-LysH$^+$ is thus *not* a simple helix. At finite T, both nonhelical and α-helical H-bond networks are competitive in energy. Our predicted structures lead to AIMD-derived anharmonic IR spectra, which match experimental IRMPD results convincingly well. In contrast, longer molecules (n = 10,15) produce similarly good IR spectra based on essentially only one conformer (α-helical). In agreement with all other evidence in the literature, these molecules are thus firmly confirmed to be α-helical in character.

EXPERIMENTAL AND COMPUTATIONAL SECTION

For the experiments, the peptides were synthesized by standard Fmoc chemistry. The experimental IRMPD spectra were recorded using the Fourier transform ion cyclotron (FT-ICR) mass spectrometer[35] at the free-electron laser FELIX.[36] Ions were brought into the gas-phase by electrospray ionization (ESI) (∼1 mg of peptide in 900 μL trifluoroacetic acid (TFA)/100 μL H_2O) and mass selected and trapped inside the ICR cell, which is optically accessible. When the IR light is resonant with an IR active vibrational mode of the molecule, many photons can be absorbed, causing the dissociation of the ion (IRMPD). Mass spectra are recorded after 4 s of IR irradiation. Monitoring the depletion of the parent ion signal and/or the fragmentation yield as a function of IR frequency leads to an IR spectrum.

All DFT+vdW calculations for this work were performed using the FHI-aims[37] program package for an accurate, all-electron description based on numeric atom-centered orbitals, with "tight" computational settings and accurate tier 2 basis sets.[37] Harmonic vibrational frequencies, intensities, and free energies were computed from finite differences. Infrared intensities $I(\omega)$ *beyond* the harmonic approximation are derived from AIMD runs > 20 ps (*NVE* ensemble, 1 fs time step, with a 300 K *NVT* equilibration), by calculating the Fourier transform of the dipole autocorrelation function[16,24,38] with a quantum correction factor to the classical line shape[39,40] proportional to ω^2 (see ref 24). To account for the spectral width of the excitation laser in the experimental setup used here, all calculated spectra (harmonic and anharmonic) are convoluted with a Gaussian broadening function with a variable width of 1% of the corresponding wavenumber. We note that further broadening mechanisms, e.g., due to the excitation process, may be reflected in the experimental

DOI: 10.1021/jz101394u | J. Phys. Chem. Lett. 2010, 1, 3465–3470

data.[25] We emphasize that the AIMD calculations presented here, at this essentially numerically converged accuracy level, are not trivial, but rather represent the computational limit of what can be done today. For example, the data shown for Ac-Ala_{15}-$LysH^+$, 180 atoms, required several days in parallel on 512 CPU cores of a new, infiniband-connected Sun Microsystems Intel Xeon (Nehalem) cluster, and are enabled only by significant parallel scalability work in FHI-aims.[37,41]

SUPPORTING INFORMATION AVAILABLE Detailed information about the H-bond pattern evolution during the AIMD run that led to the calculated anharmonic spectra for Ac-Ala_{15}-$LysH^+$ in Figure 1c. This material is available free of charge via the Internet at http://pubs.acs.org/.

AUTHOR INFORMATION

Corresponding Author:

*To whom correspondence should be addressed. E-mail: rossi@fhi-berlin.mpg.de.

Present Addresses:

§ Current address: University of Oxford, Chemistry Research Laboratory, Mansfield Road, Oxford OX1 3TA, U.K.

ACKNOWLEDGMENT We gratefully acknowledge the support by the "Stichting voor Fundamenteel Onderzoek der Materie" (FOM) in providing the required beam time on FELIX and highly appreciate the skillful assistance by the FELIX staff, in particular Dr. B. Redlich and Dr. A. F. G. van der Meer. We also acknowledge funding by the European Theoretical Spectroscopy Facility e-Infrastructure (Grant No. 211956).

REFERENCES

(1) Benesch, J.; Robinson, C. Biological Chemistry: Dehydrated but Unharmed. *Nature* **2009,** *462*, 576–577.
(2) Wu, Q.; Yang, W. Empirical Correction to Density Functional Theory for van der Waals Interactions. *J. Chem. Phys.* **2002,** *116*, 515–524.
(3) Dion, M.; Rydberg, H.; Schröder, E.; Langreth, D. C.; Lundqvist, B. I. van der Waals Density Functional for General Geometries. *Phys. Rev. Lett.* **2004,** *92*, 246401.
(4) Jurecka, P.; Czerny, J.; Hobza, P.; Salahub, D. R. Density Functional Theory Augmented with an Empirical Dispersion Term. Interaction Energies and Geometries of 80 Noncovalent Complexes Compared with Ab Initio Quantum Mechanics Calculations. *J. Comput. Chem.* **2006,** *28*, 555–569.
(5) Grimme, S.; Antony, J.; Schwabe, T.; Mück-Lichtenfeld, C. Density Functional Theory with Dispersion Corrections for Supramolecular Structures, Aggregates, and Complexes of (Bio)organic Molecules. *Org. Biomol. Chem.* **2007,** *5*, 741–758.
(6) Tkatchenko, A.; Scheffler, M. Accurate Molecular van der Waals Interactions from Ground-State Electron Density and Free-Atom Reference Data. *Phys. Rev. Lett.* **2009,** *102*, 073005. Some of the present calculations for the small Ala_5 helices employ an early version of this scheme, which yields the same geometries and energetics within less than 10 meV as the final scheme of Tkatchenko and Scheffler .
(7) Lee, K.; Murray, E. D.; Kong, L.; Lundqvist, B. I.; Langreth, D. C. Higher-Accuracy van der Waals Density Functional. *Phys. Rev. B* **2010,** *82*, 081101.
(8) Hudgins, R. R.; Ratner, M. A.; Jarrold, M. F. Design of Helices That Are Stable in Vacuo. *J. Am. Chem. Soc.* **1998,** *120*, 12974–12975.
(9) Hudgins, R. R.; Jarrold, M. F. Helix Formation in Unsolvated Alanine-Based Peptides: Helical Monomers and Helical Dimers. *J. Am. Chem. Soc.* **1999,** *121*, 3494–3501.
(10) Kohtani, M.; Kinnear, B. S.; Jarrold, M. F. Metal-Ion Enhanced Helicity in the Gas Phase. *J. Am. Chem. Soc.* **2000,** *122*, 12377–12978.
(11) Kohtani, M.; Jarrold, M. F. Water Molecule Adsorption on Short Alanine Peptides: How Short Is the Shortest Gas-Phase Alanine-Based Helix? *J. Am. Chem. Soc.* **2004**, *126*, 8454−8458.
(12) Kohtani, M.; Jarrold, M. F.; Wee, S.; O'Hair, R. A. J. Metal Ion Interactions with Polyalanine Peptides. *J. Phys. Chem. B* **2004,** *108*, 6093–6097.
(13) Stearns, J. A.; Boyarkin, O. V.; Rizzo, T. R. Spectroscopic Signatures of Gas-Phase Helices: Ac-Phe-$(Ala)_5$-Lys-H^+ and Ac-Phe-$(Ala)_{10}$-Lys-H^+. *J. Am. Chem. Soc.* **2007,** *129*, 13820–13821.
(14) Stearns, J. A.; Seaiby, C.; Boyarkin, O. V.; Rizzo, T. R. Spectroscopy and Conformational Preferences of Gas-Phase Helices. *Phys. Chem. Chem. Phys.* **2009,** *11*, 125–132.
(15) Vaden, T. D.; de Boer, T. S. J. A.; Simons, J. P.; Snoek, L. C.; Suhai, S.; Paizs, B. Vibrational Spectroscopy and Conformational Structure of Protonated Polyalanine Peptides Isolated in the Gas Phase. *J. Phys. Chem. A* **2008,** *112*, 4608–4616.
(16) Cimas, A.; Vaden, T. D.; de Boer, T. S. J. A.; Snoek, L. C.; Gaigeot, M.-P. Vibrational Spectra of Small Protonated Peptides from Finite Temperature MD Simulations and IRMPD Spectroscopy. *J. Chem. Theory Comput.* **2009,** *5*, 1068–1078.
(17) Perdew, J. P.; Burke, K.; Ernzerhof, M. Generalized Gradient Approximation Made Simple. *Phys. Rev. Lett.* **1996,** *77*, 3865–3868.
(18) Mortenson, P.; Evans, D.; Wales, D. Energy Landscapes of Model Polyalanines. *J. Chem. Phys.* **2002,** *117*, 1363–1377.
(19) Pendry, J. Reliability Factors for LEED Calculations. *J. Phys. C: Solid State Phys.* **1980,** *13*, 937–944.
(20) Hove, M. V.; Weinberg, W.; Chan, C. *Low-Energy Electron Diffraction*; Springer-Verlag: Berlin, 1986.
(21) Blum, V.; Heinz, K. Fast LEED Intensity Calculations for Surface Crystallography Using Tensor LEED. *Comput. Phys. Commun.* **2001,** *134*, 392–425.
(22) Oboodi, M. R.; Alva, C.; Diem, M. Solution-Phase Raman Studies of Alanyl Dipeptides and Various Isotopomers: A Reevaluation of the Amide III Vibrational Assignment. *J. Phys. Chem.* **1984,** *88*, 501–505.
(23) Weymuth, T.; Jacob, C. R.; Reiher, M. A Local-Mode Model for Understanding the Dependence of the Extended Amide III Vibrations on Protein Secondary Structure. *J. Phys. Chem. B* **2010,** *114*, 10649–10660.
(24) Gaigeot, M.-P.; Martinez, M.; Vuilleumier, R. Infrared Spectroscopy in the Gas and Liquid Phase from First Principle Molecular Dynamics Simulations: Application to Small Peptides. *Mol. Phys.* **2007**, *105*, 2857−2878, and references therein.
(25) Oomens, J.; Sartakov, B. G.; Meijer, G.; von Helden, G. Gas-Phase Infrared Multiple Photon Dissociation Spectroscopy of Mass-Selected Molecular Ions. *Int. J. Mass Spectrom.* **2006,** *254*, 1–19.
(26) Kohtani, M.; Jones, T. C.; Schneider, J. E.; Jarrold, M. F. Extreme Stability of an Unsolvated α-Helix. *J. Am. Chem. Soc.* **2004,** *126*, 7420–7421.
(27) Tkatchenko, A.; Rossi, M.; Blum, V.; Scheffler, M., submitted for publication in *Phys. Rev. Lett.*, 2010.

(28) Price, M.; Dennis, O.; William, J. Gas-Phase and Liquid-State Properties of Esters, Nitriles, and Nitro Compounds with the OPLS-AA Force Field. *J. Comput. Chem.* **2001,** *22*, 1340–1352.
(29) TINKER - Software Tools for Molecular Design, http://dasher.wustl.edu/tinker, version 4.2, downloaded in March 2008. We used the *opls-aa* force field parameters distributed with this version of the program.
(30) Beachy, M. D.; Chasman, D.; Murphy, R. B.; Halgren, T. A.; Friesner, R. A. Accurate Ab Initio Quantum Chemical Determination of the Relative Energetics of Peptide Conformations and Assessment of Empirical Force Fields. *J. Am. Chem. Soc.* **1997,** *119*, 5908–5920.
(31) Kaminski, G. A.; Friesner, R. A.; Tirado-Rives, J.; Jorgensen, W. L. Evaluation and Reparametrization of the OPLS-AA Force Field for Proteins via Comparison with Accurate Quantum Chemical Calculations on Peptides. *J. Phys. Chem. B* **2001,** *105*, 6474–6487.
(32) Penev, E.; Ireta, J.; Shea, J.-E. Energetics of Infinite Homopolypeptide Chains: A New Look at Commonly Used Force Fields. *Phys. Chem. B* **2008,** *112*, 6872–6877.
(33) As an additional test, to rule out any unexpected effect from geometry changes due to different functionals, we fully relaxed the α-1 geometry with the B3LYP functional. The result is very similar to the fully relaxed PBE geometry.
(34) Wyttenbach, T.; von Helden, G.; Batka, J. J., Jr.; Carlat, D.; Bowers, M. T. Effect of the Long-Range Potential on Ion Mobility Measurements. *J. Am. Soc. Mass Spectrom.* **1997,** *8*, 275–282.
(35) Valle, J.; Eyler, J.; Oomens, J.; Moore, D.; Meer, A.; von Helden, G.; Meijer, G.; Hendrickson, C.; Marshall, A.; Blakney, G. Free Electron Laser—Fourier Transform Ion Cyclotron Resonance Mass Spectrometry Facility for Obtaining Infrared Multiphoton Dissociation Spectra of Gaseous Ions. *Rev. Sci. Instrum.* **2005,** *76*, 023103.
(36) Oepts, D.; van der Meer, A.; van Amersfoort, P. The Free-Electron-Laser User Facility FELIX. *Infrared Phys. Technol.* **1995,** *36*, 297–308.
(37) Blum, V.; Gehrke, R.; Hanke, F.; Havu, P.; Havu, V.; Ren, X.; Reuter, K.; Scheffler, M. Ab Initio Molecular Simulations with Numeric Atom-Centered Orbitals. *Comput. Phys. Commun.* **2009,** *180*, 2175–2196.
(38) Li, X.; Moore, D. T.; Iyengar, S. S. Insights from First Principles Molecular Dynamics Studies toward Infrared Multiple-Photon and Single-Photon Action Spectroscopy: Case Study of the Proton-Bound Dimethyl Ether Dimer. *J. Chem. Phys.* **2008,** *128*, 184308.
(39) Borysow, J.; Moraldi, M.; Frommhold, L. The Collision Induced Spectroscopies. *Mol. Phys.* **1985,** *56*, 913–922.
(40) Ramirez, R.; Lopez-Ciudad, T.; Kumar, P.; Marx, D. Quantum Corrections to Classical Time-Correlation Functions: Hydrogen Bonding and Anharmonic Floppy Modes. *J. Chem. Phys.* **2004,** *121*, 3973–3983.
(41) Havu, V.; Blum, V.; Havu, P.; Scheffler, M. Efficient O(N) Integration for All-Electron Electronic Structure Calculation Using Numeric Basis Functions. *J. Comput. Phys.* **2009,** *228*, 8367–8379.

DOI: 10.1021/jz101394u | *J. Phys. Chem. Lett.* **2010,** *1*, 3465–3470